Structural relaxation in chalcogenide-based phase change memories (PCMs): from defect-annihilation kinetic to device-reliability prediction

S. Lavizzari, D. Ielmini, D. Sharma and A. L. Lacaita
Dipartimento di Elettronica e Informazione, Politecnico di Milano and IU.NET
20133 Milano, Italy, Tel. +39 02 2399 4007, Email: lavizzari@elet.polimi.it

ABSTRACT

Chalcogenide glasses, widely used in phase change memories, are unstable versus both structural relaxation (SR) and crystallization. SR is a thermally-activated, atomistic-scale reassessment of the amorphous structure. While crystallization leads to a decrease of resistance with time, SR results in a resistance increase (drift). Although both phenomena affect phase-change memory (PCM) reliability, SR mechanism is still not fully understood. Here we address SR physics by electrical measurements of PCM cells, providing a physics-based model for drift and the optimization of the cell readout condition to minimize the reliability impact of drift.

Key words: Amorphous semiconductors, chalcogenide, phase-change memory (PCM), non volatile memories, structural relaxation.

1. INTRODUCTION

After the original proposal of the reversible switching processes by Ovshinsky [1], the memory industry has carried on an intense research on phase change memory (PCM) cells [2-8]. In particular, these efforts have seen a strong increase in the last decade, to provide a feasible alternative to Flash non-volatile memories. In fact, while Flash will certainly face serious reliability and scaling limitations beyond the 45 nm node, the PCM concept features instead extended endurance, good data retention and almost ideal scaling behavior [9].
In order to provide good reliability it is necessary to understand the physics of conduction and phase transition phenomena. This work will address the physical interpretation and modeling of structural relaxation (SR) in GST-based PCM devices. SR is a local rearrangement of the amorphous structure due to atomic motion, in order to gain a more favorable thermodynamic equilibrium state. First, the nature of SR phenomena is studied by a literature survey on SR effects in metallic glasses and amorphous semiconductors (Si, Ge and several chalcogenide compounds). From this analysis, the experimental features of SR can be generally described in terms of a defect (e.g. locally distorted bonds, dangling bonds and so on) annihilation process [10-12]. More evidence for defect annihilation as a root cause for SR effects in amorphous GST will be gained from electrical measurements on PCM cells. Based on this physical interpretation, a kinetic model for defect annealing in the amorphous GST is developed, assuming an Arrhenius decay law with broad distribution of activation energies [13-15]. The defect kinetic will then be linked to the electrical behavior of amorphous GST through a thermally-assisted hopping model for conduction through localized states [16]. Extensive comparison with electrical data will be shown, allowing to validate the physical model and minimize the impact of SR on PCM reliability.

2. MODELING THE STRUCTURAL RELAXATION

It is well know that the crystalline phase possesses a good stability, while the amorphous one is metastable, and can experience both crystallization [17], [18], and structural relaxation (SR) [19]. SR consists in the atomistic-level rearrangement of the disorder structure, which spontaneously evolves into an amorphous phase with higher thermodynamic stability, in order to minimize Gibbs free energy [19], [20]. SR has not to be considered like a phase transition, it can be described as a short range ordering process, while a substantial disorder is still kept on the long range [10]. Diffraction analysis shows that the structure remains disordered in the long range, with negligible change of the distance between first-nearest-neighbor atoms and an increase in the connectivity of the amorphous network

[10], [23]. SR plays an important role in modifying the electrical properties of the chalcogenide material, e.g. resistance and threshold voltage [19], contributing to the reliability issues of the memory device. In order to predict data retention in PCM devices, a careful study of SR mechanisms in mandatory, both in time and temperature [20], [21]. SR itself is not a new concept, it was previously reported by physical analysis for several amorphous materials, including metallic glasses [13], Si [10], Ge [22], SiC [23], Se [24], [12] and phase-change chalcogenide materials [25]. Calorimetric measurements performed on materials listed above show energy release during SR, supporting the theory that SR is an exothermic process that brings the amorphous metastable state towards a more stable one [10], [22], [25]. These evidences indicate that SR consists of a defect annihilation process within the amorphous structure [10], [12]. A change in defects concentration can affect the conduction and the switching properties of the chalcogenide material since electrical conduction in the amorphous phase is due to thermally-activated hopping through localized states [26-29].

To describe the SR kinetic we refer to the physical interpretation in which SR effects where explained by a defect annihilation process in the amorphous chalcogenide. With the term defects we refer here to dangling bonds, local bond distortions by angle and/or length, vacancies, compositional disorder in the amorphous structure and so on [10], [22]. Defects are modeled as metastable states in the disordered amorphous structure, as schematically shown in Fig. 1 for a dangling bond. In order to model the evolution of the metastable state, we applied the concept of double well potential, well known in literature to describe a system in which there are two thermo-dynamical states with different free energy associated [31], [32].The metastable state can relax to an equilibrium state by thermal excitation over an energy barrier E_A with an average reaction time τ, assumed to depend on temperature T according to the classical Arrhenius law [13], [20], [30]:

$$\tau = \tau_{at} e^{\frac{E_A}{k_B T}} \tag{1}$$

where τ_{at} is a typical time constant for atomic vibration, k_B is the Boltzmann constant and E_A is the barrier height for relaxation, acting as an activation energy for the process. An atomic time $\tau_{at}=10^{-13}$s was assumed, in agreement with typical phonon vibration time [28], [30].

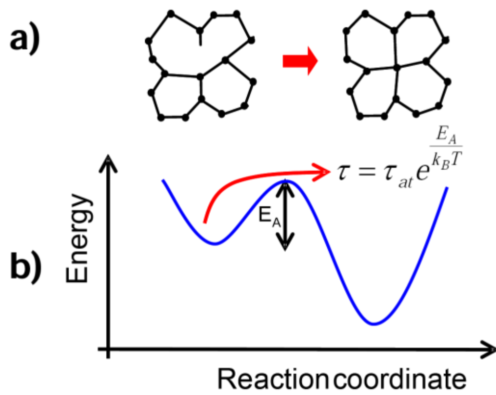

Fig. 1 Kinetic model for SR in chalcogenide glasses. Metastable states are healed (a) by thermal excitation over an energy barrier E_A (b).

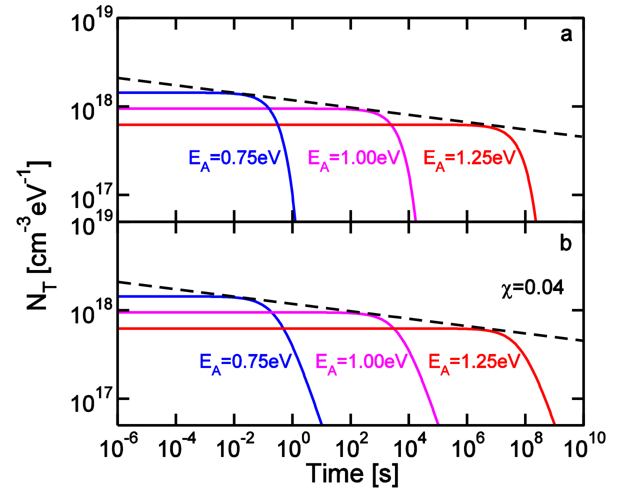

Fig. 2 Calculated evolution of N_T at three different energies E_A = 0.75, 1 and 1.25eV . Summation over all energies yields a power law, where the exponent is independent of the kinetics assumed: monomolecular (a), bimolecular (b).

As already pointed out, a broad distribution of activation energies [13-15] is needed in order to explain the large scale of times, from ns up to weeks, in which the change in electrical properties is observed [3], because the characteristic time of the evolution of the system is related from Eq. (1) to the activation energy E_A. Also, we assumed that the initial (i.e. before any annihilation event) distribution of traps $N_T(E_A,t)$ [cm^{-3}eV^{-1}] depends exponentially on E_A, according to:

$$N_T\left(E_A,0\right)=\frac{N_{tot}}{\sigma}e^{-\frac{E_A}{\sigma}} \tag{2}$$

where N_{tot} [cm^{-3}] is the total concentration of traps and σ [eV] is an energy decay constant that models the distribution. In order to give reason of the previous evidence [12], in which there was shown that in a chalcogenide glass the concentration of defects decrease with time like a power-law, we chose an exponential dependence on energy. However, our SR model can be applied to other shapes of energy distribution.

To describe the evolution with time of the defects concentration, different reaction kinetics are possible: in particular, a monomolecular reaction kinetics [13], [20] and a bimolecular reaction kinetics [10], [11] were proposed. Roorda et al. [10] have explained the monomolecular defect annihilation by defect flow and disappearance in traps, while the bimolecular dynamics was explained by defects annihilating in pairs.

Integration in energy and time both the kinetics, in combination with Eq. (1) and Eq. (2), yields to power-law time-dependence of the total trap density as previously observed by experiments [12]:

$$N_{tot}(t)=N_{tot,0}\left(\frac{t}{t_0}\right)^{-\chi} \tag{5)3$$

Where $N_{tot,0}$ and t_0 are constants and the exponent is $\chi = k_BT/\sigma$. The N_{tot}-t behavior is controlled by the relation between τ and E_A. This is shown in Fig. 2. The figure shows the calculated time evolution of N_T for three energy levels, namely E_A = 0.75, 1.00, 1.25eV and for either a monomolecular (a) or a bimolecular (b) reaction kinetics. In both figures, N_T remains constant up to a characteristics time, then displays a drop. The envelope of the $N_T(E_A)$-t curves gives the power-law for N_{tot}. From the figure it is also appreciable that the order of the kinetic doesn't affect the final N_{tot}-t law. Thus, defect decay measurements alone can hardly reveal the order of the SR reaction kinetics.

3. IMPACT OF SR ON ELECTRICAL PROPERTIES

The resistance of the amorphous phase is not constant in time, as clearly visible in Fig. 3. It increases with time, following the equation:

$$R(t)=R_0\left(\frac{t}{t_0}\right)^{\nu} \tag{7)4$$

Where R_0 is the initial programmed resistance at the initial programming time t_0. ν was found to be in the range of 0.10 ± 0.1 at room temperature.

Carefully examination of the I-V curves in Fig. 4 indicates that not only R at low voltage, but also the sub-threshold slope (STS, see inset) increases with time due to the SR. To consistently account for the concomitant drift of R and STS, we refer to the trap-limited conduction model in the amorphous phase [16]. Carriers are thermally emitted from one trap to the other, with average spacing Δz and energy barrier $E_C - E_F$. Application of a bias V results in a barrier lowering, leading to a current I given by:

$$I=2qAN_{tot}\frac{\Delta z}{\tau_0}e^{\frac{E_C-E_F}{k_BT}}Sh\left(\frac{qV\Delta z}{2k_BTu_a}\right) \tag{8)5$$

Where A is the area, N_{tot} the total trap density, Δz is the average distance between traps, $\tau_0 = 10^{-15}$s is the attempt to escape time, E_C is conduction edge level, E_F is the Fermi level, V is the applied voltage and u_a is the amorphous thickness.

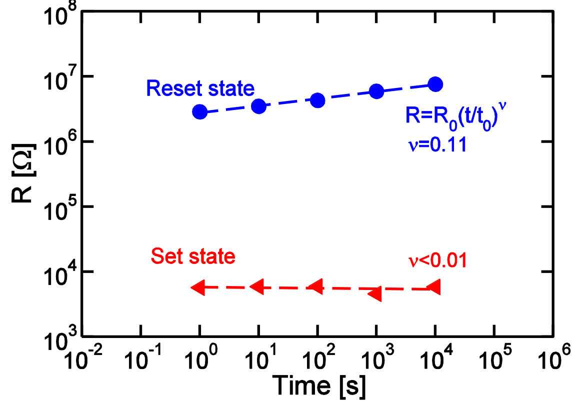

Fig. 3 Measured resistance versus time. While the crystalline phase shows a constant resistance, the amorphous one displays a resistance drift, governed by a power-law and due to structural relaxation (SR).

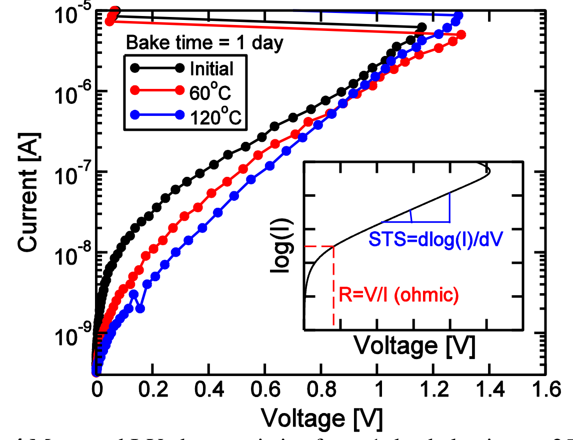

Fig. 4 Measured I-V characteristic after a 1 day bake time at 25, 60 and 120°C. Both low field resistance and sub-threshold slope (STS) increases with the increasing bake temperature. The inset shows the definition of the STS. Measurement was carried out at room temperature.

The low field resistance R and the sub-threshold slope STS can be derived from Eq. (5), leading to:

$$R = \frac{k_B T u_a \tau_0}{q^2 A N_{tot} \Delta z^2} e^{-\frac{E_C - E_F}{k_B T}} \tag{9)6$$

$$STS = \frac{d \log I}{dV} = \frac{q \Delta z}{2 k_B T u_a} \tag{10)7$$

Since Δz is the average distance between defects, a decreasing of N_{tot} due to SR in the material and a consequent increase of Δz, leads to an increase of both R and STS [20].

Given the exponential dependence of R on the mobility edge (E_C-E_F), this effect is believed to play the most important role in the change of resistance during SR. A similar change in the mobility edge results in a variations in the threshold voltage V_T [16]. As a result, also the threshold voltage increase with time due to SR. The shift of the mobility edge towards higher energy is due to a change of DOS during SR or to consider a change in Coulombic lowering of the hopping barrier for increasing trap distance. A similar change in the mobility edge for holes can be assumed.

The combination of the kinetic model for defect annihilation with the hopping conduction model allows to comprehensively account for the time evolution of electrical parameters of the cell for device reliability assessment. Fig. 5 shows measured and calculated resistance as a function of annealing time. Annealing was performed at two different temperatures 50 and 100°C, while resistance measurement was performed at room temperature. Data were obtained for a GST-based PCM cell in the reset state. The calculation in the figure was obtained assuming an exponential distribution of traps with σ = 0.6eV, as shown in Fig. 6a. Here, the evolution of the energy distribution of traps is shown for increasing times (t = 10^{-4}, 0.3, 700 and 2×10^6s) during the relaxation process. For any relaxation time t*, the concentration of traps having energies below a characteristic E* is largely suppressed, whereas above this level the distribution remains unaffected. This can be viewed as a shift of an annealing front to increasing energy. The characteristic energy defining the position of the annealing front with time can be obtained as the energy for which trap states have decayed by a factor *e*, from Eq. (1) $E^* = k_B T \exp(t^*/\tau_{at})$. Note that the simulation results for R indicate a power-law increase, as expected from Fig. 3.

Moreover at higher temperatures the annealing front shifts toward higher energies at fixed annealing time (Fig. 6b). This is a natural consequence of the activation with temperature (see the equation for E*) and reflects also in the drift behavior as we will point out in the next section.

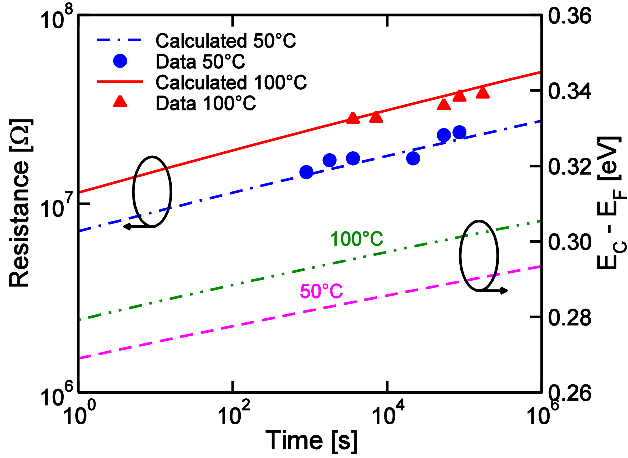

Fig. 5 Calculated R and E_C-E_F as a function of time, for T = 50 and 100°C. The figure also shows measured R for a GST-based PCM cell. Data are in good agreement with the simulations.

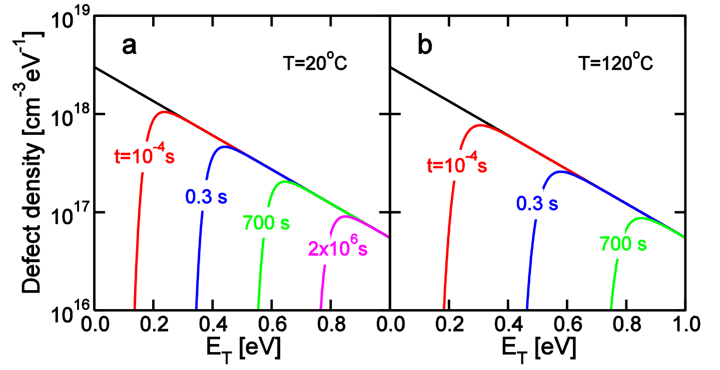

Fig. 6 Simulated evolution of N_T at different times for 20 (a) and 120°C(b). The figure shows the annealing "fronts" as a function of time and the correspondent density of defects annealed. Note that higher is T, higher is the speed of these "fronts".

4. TEMPERATURE EFFECTS AND RELIABILTY

The comparison of the calculated R in Fig. 5 shows that ν increase for increasing annealing temperatures. This can be understood by the thermal activation of the relaxation process as shown by Eq. (1). To better show the effect of temperature on SR, Fig. 7 shows measured and calculated R (a) and STS (b), after annealing at increasing temperature T in the range 40 to 120°C. A constant annealing time of one day was used, while both R and STS were measured at room temperature. Calculations by our numerical model consistently account for measured results. In particular, it should be noted that, although the analytical model in Eq. (5) describes hopping transport in presence of a large trap density (small Δz), its results can provide a reasonable prediction of both R and STS. In particular, the STS increase with annealing temperature can be explained by the linear relation with Δz in Eq. (7). The increase of R is instead mainly resulting from the increase of mobility edge, as already discussed.

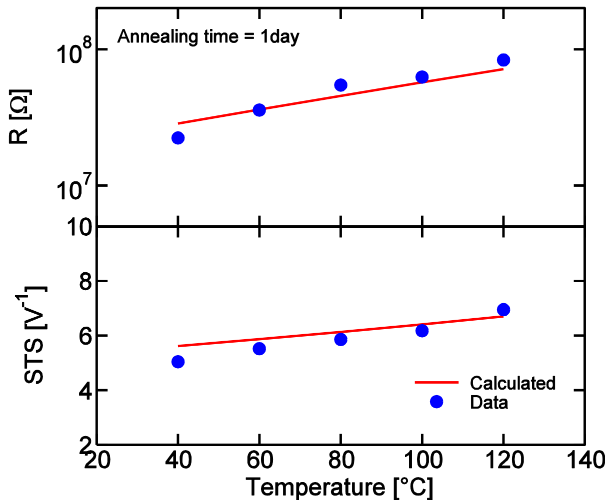

Fig. 7 Measured and calculated R(a) and STS (b), as a function of the temperature of a one-day annealing.

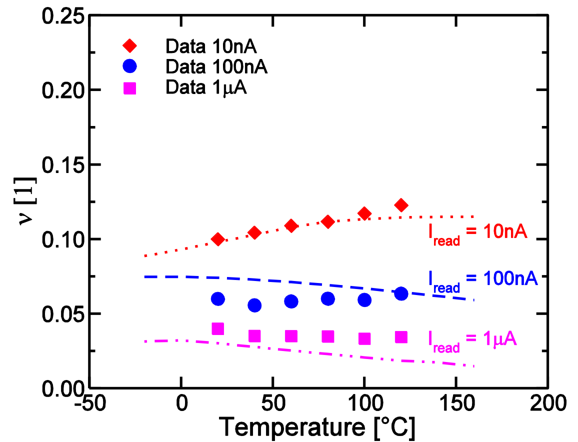

Fig. 8 Measured (symbols) and calculated (lines) ν as a function of temperature and for increasing read currents I_{read} = 1nA, 100nA and 1µA.

From a device point of view, the most relevant parameter describing the evolution of R with time for different temperatures and read conditions is the exponent ν in the power law of Eq. (4). Fig. 8 shows measured and calculated

ν as a function of T and for increasing read current I_{read} = 1nA, 100nA and 1μA. From Fig. 8 it is evident that ν increases for increasing T, as a result of the activation in temperature of SR (see Eq. 1). On the other hand ν decreases with I_{read}, as a result of a) the exponential increase of current with voltage and b) the increase of average STS during SR as a result of defect annihilation (see also Fig. 7). Simulation results in the figure successfully account for the dependence of ν on both T and I_{read}. This result can suggest a methodology to reduce the impact of the drift on the device reliability: Reading at relatively high current could have a beneficial effect on R stability with time.

5. CONCLUSIONS

A new physical interpretation and model for drift in PCM based on structural relaxation is provided. A defect annihilation model, combined with a Poole-Frenkel conduction model accounts for R, STS, and ν as a function of time, temperature and read current. The model is also consistent with all the measurements performed and with the recently proposed switching model based on Poole-Frenkel conduction. Optimization of read conditions by high I_{read} is finally suggested to maximize R stability in the PCM devices.

REFERENCES

[1] S. R. Ovshinsky, "Reversible electrical switching phenomena in disordered structures," Phys. Rev. Lett., vol. 21, pp. 1450–1453, 1968.

[2] S. J. Ahn, Y. J. Song, C. W. Jeong, J. M. Shin, Y. Fai, Y. N. Hwang, S. H. Lee, K. C. Ryoo, S. Y. Lee, J. H. Park, H. Horii, Y. H. Ha, J. H. Yi, B. J. Kuh, G. H. Koh, G. T. Jeong, H. S. Jeong, K. Kim, and B. I. Ryu, "Highly manufacturable high density phase change memory of 64 Mb and beyond," in IEDM Tech. Dig., pp. 907–910, 2004.

[3] F. Pellizzer, A. Benvenuti, B. Gleixner, Y. Kim, B. Johnson, M. Magistretti, T. Marangon, A. Pirovano, R. Bez, and G. Atwood, "A 90nm phase change memory technology for stand-alone non-volatile memory applications," in Symp. on VLSI Tech. Dig., pp. 122–123, 2006.

[4] Y. N. Hwang, S. H. Lee, S. J. Ahn, S. Y. Lee, K. C. Ryoo, H. S. Hong, H. C. Koo, F. Yeung, J. H. Oh, H. J. Kim, W. C. Jeong, J. H. Park, H. Horii, Y. H. Ha, J. H. Yi, G. H. Koh, G. T. Jeong, H. S. Jeong, and K. Kim, "Writing current reduction for high-density phase change PRAM," in IEDM Tech. Dig., pp. 893–896, 2003.

[5] F. Pellizzer, A. Pirovano, F. Ottogalli, M. Magistretti, M. Scaravaggi, P. Zuliani, M. Tosi, A. Benvenuti, P. Besana, S. Cadeo, T. Marangon, R. Morandi, R. Piva, A. Spandre, R. Zonca, A. Modelli, E. Varesi, T. Lowrey, A. Lacaita, G. Casagrande, P. Cappelletti, and R. Bez, "Novel μtrench phase-change memory cell for embedded and stand-alone nonvolatile memory applications," in Symp. on VLSI Tech. Dig., pp. 18–19, 2004.

[6] M. H. Lankhorst, B. W. Ketelaars, and R. Wolters, "Low-cost and nanoscale non-volatile memory concept for future silicon chips," Nature, vol. 236, pp. 36–49, 2005.

[7] F. Merget, D. H. Kim, P. H. Bolivar, and H. Kurz, "Lateral phase change random access memory cell design for low power operation," Microsyst. Technol., vol. 13, no. 2, pp. 169–172, 2006.

[8] Y. C. Chen et al., "Ultra-thin phase-change bridge memory device using GeSb," in IEDM Tech. Dig., pp. 777–780, 2006.

[9] S. Lai, "Current status of the phase change memory and its future," in IEDM Tech. Dig, pp. 255–258, 2003.

[10] S. Roorda, W. C. Sinke, J. M. Poate, D. C. Jacobson, S. Dierker, B. S. Dennis, D. J. Eaglesham, F. Spaepen and P. Fuoss, "Structural relaxation and defect annihilation in pure amorphous silicon", Phys. Rev. B, 1991, 44, pp. 3702-3725.

[11] J. Kalb, F. Spaepen, T. P. Leevard Pedersen and M. Wuttig, "Viscosity and elastic constants of thin films of amorphous Te alloys used for optical data storage", J. Appl. Phys., 2003, 94, pp. 4908-4912.

[12] K. Koughia, Z. Shakoor, S. O. Kasap, and J. M. Marshall, “Density of localized electronic states in a-Se from electron time-of-flight photocurrent measurements”, J. Appl. Phys., 2005, 97, pp. 3706–3716.

[13] Khonik, K. Kitagawa and H. Morii, “On the determination of the crystallization activation energy of metallic glasses”, J. Appl. Phys., 2000, 87, pp. 8440-8443.

[14] O. Penzin, A. Haggag, W. McMahon, E. Lyumkis, K. Hess, “MOSFET degradation kinetics and its simulations”, IEEE Trans. On El. Dev., Vol. 50, No. 6, pp. 1445-1450, 2003.

[15] G. Schumm, G. H. Bauer, “Energy resolved defect in a-Si:H investigated by modulated photocurrent”, IEEE, pp. 154-159, 1988.

[16] D. Ielmini and Y. Zhang, “Analytical model for subthreshold conduction and threshold switching in chalcogenide-based memory devices”, J. Appl. Phys., 2007, 102, 054517.

[17] U. Russo, D. Ielmini, A. Redaelli, and A. L. Lacaita, “Intrinsic data retention in nanoscaled PCMs – Part I: Monte Carlo model for crystallization and percolation,” IEEE Trans. Electron Devices, vol. 53, pp. 3032–3039, 2006.

[18] A. Redaelli, D. Ielmini, U. Russo, and A. L. Lacaita, “Intrinsic data retention in nanoscaled PCMs – Part II: Statistical analysis and prediction of failure time,” IEEE Trans. Electron Devices, vol. 53, pp. 3040–3046, 2006.

[19] D. Ielmini, A. L. Lacaita, and D. Mantegazza, “Recovery and drift dynamics of resistance and threshold voltages in phase-change memories,” IEEE Trans. Electron Devices, vol. 54, pp. 308–315, 2007.

[20] D. Ielmini, S. Lavizzari, D. Sharma, and A. L. Lacaita, “Physical interpretation, modeling and impact on phase change memory (PCM) reliability of resistance drift due to chalcogenide structural relaxation,” in IEDM Tech. Dig., 2007, pp. 939–942.

[21] T. Nirschl, J. B. Philipp, T. D. Happ, G. W. Burr, B. Rajendran, M.- H. Lee, A. Schrott, M. Yang, M. Breitwisch, C.-F. Chen, E. Joseph, M. Lamorey, R. Cheek, S.-H. Chen, S. Zaidi, S. Raoux, Y. Chen, Y. Zhu, R. Bergmann, H.-L. Lung, and C. Lam, “Write strategies for 2 and 4-bit multi-level phase-change memory,” in IEDM Tech. Dig., 2007.

[22] E. P. Donovan, F. Spaepen, D. Turnbull, J. M. Poate, and D. C. Jacobson, “Calorimetric studies of crystallization and relaxation of amorphous Si and Ge prepared by ion implantation,” J. Appl. Phys., vol. 57, pp. 1795– 1804, 1985.

[23] M. Hishimaru, I.-T. Bae, Y. Hirotsu, S. Matsumura, and K. E. Sickafus, “Structural relaxation of amorphous silicon carbide,” Phys. Rev. Lett., vol. 89, p. 055502, 2002.

[24] S. O. Kasap and S. Yannacopoulos, “Kinetics of structural relaxations in glassy semiconductor a-Se,” J. Mater. Res., vol. 4, pp. 893–905, 1989.

[25] J. A. Kalb, M. Wuttig, and F. Spaepen, “Calorimetric measurements of structural relaxation and glass transition temperatures in sputtered films of amorphous Te aloys used for phase change recording,” J. Mater. Res., vol. 22, pp. 748–754, 2007.

[26] D. Emin, “Current-driven threshold switching of a small polaron semiconductor to a metastable conductor,” Phys. Rev. B, vol. 74, p. 035206, 2006.

[27] D. Ielmini and Y. Zhang, “Evidence for trap-limited transport in the subthreshold conduction regime of chalcogenide glasses,” Appl. Phys. Lett., vol. 90, p. 192102, 2007.

[28] N. F. Mott and E. A. Davis, Electronic processes in non-crystalline materials. Clarendon Press, Oxford, 1979.

[29] D. Ielmini, “Threshold switching mechanism by high-field energy gain in the hopping transport of chalcogenide glasses”, Phys. Rev. B 78, 035308, 2008.

[30] D. Ielmini, S. Lavizzari, D. Sharma and A. L. Lacaita, "Temperature acceleration of structural relaxation in amorphous Ge2Sb2Te5", Appl. Phys. Lett. 92, 193511, 2008.

[31] C. A. Angell, et al., "Relaxation in glassforming liquids and amorphous solids", Appl. Phys. Rev., Vol. 88, No. 6, pp. 3113-3157, 2000.

[32] A. Witvrouv and F. Spaepen, "Viscosity and elastic constants of amorphous Si and Ge", J. Appl. Phys. 74, pp. 7154-7161, 1993.

Biographies

Simone Lavizzari was born in 1982 in Milano, Italy. He took the first level Laurea (Bachelor) degree with first class honors in 2004, and the second level Laurea (Master) degree with first class honors in 2006, both in electrical engineering at the Politecnico di Milano, Italy. For his first level graduation thesis he worked on low temperature electronics (4.2K – 100K), within the Department of Nuclear Engineering of Politecnico di Milano, Italy. For his second level graduation thesis he worked on Phase Change Memories (PCMs) within the Department of Electrical Engineering of Politecnico di Milano, Italy, where he is currently taking his PhD degree. His research interests include the modeling of electrical and physical properties in PCM devices and the design of VLSI analog instrumentation for biological characterizations.